



# Single nucleotide polymorphism detection method by temperature-gradient affinity chromatography using a single-stranded oligo-DNA coupled column

Katsuda, Tomohisa

Nishijima, Ken

Kamura, Mitsumasa

Nishiwada, Yasushi

Kato, Shigeo

---

## (Citation)

Journal of Chromatography A, 1123(2):182-188

## (Issue Date)

2006-08-11

## (Resource Type)

journal article

## (Version)

Accepted Manuscript

## (URL)

<https://hdl.handle.net/20.500.14094/90000289>



**Single nucleotide polymorphism detection method by temperature-gradient  
affinity chromatography  
using a single-stranded oligo-DNA coupled column**

Tomohisa Katsuda, Ken Nishijima, Mitsumasa Kamura, Yasushi Nishiwada and Shigeo  
Katoh\*

Graduate School of Science and Technology, Kobe University, 657-8501 Kobe, Japan

\* Corresponding author

Tel. & Fax. +81-78-803-6193

e-mail [katoh@kobe-u.ac.jp](mailto:katoh@kobe-u.ac.jp)

## **Abstract**

We developed an affinity chromatographic method for simple SNP (single nucleotide polymorphism) detection by use of a single-stranded DNA-coupled column and temperature gradient elution, utilizing the difference in thermal stability between hybridized double-stranded DNAs with and without mismatched base-pairs in the course of temperature gradient elution. We studied experimentally and theoretically the elution behavior of DNAs with and without SNPs in this chromatography and proposed a numerical calculation method based on a thermodynamic dissociation model. The effects of the column volume, flow rate of eluent and heating rate of the column on elution profiles were clarified. For designing DNA ligands, mismatched base-pair positions favorable for detection of SNPs were also explored by use of hybridized DNAs coding a part of the human TP53 gene.

*Key words:* SNP detection; DNA coupled column; Affinity chromatography; Temperature gradient elution; Thermodynamic dissociation model; TP53 gene

## **1. Introduction**

Minor genetic variations, particularly single nucleotide polymorphism (SNP) found in specific positions of the human genome, have extensively been studied to understand gene functions related to inheritable diseases [1] and individual differences in susceptibility to diseases and drugs [2]. SNP detection methods have been developed for two purposes. To clarify many phenotypes of SNPs, intensive screening of a huge number of samples is necessary, such as in the case of DNA micro-array systems. On the other hand, to detect specific SNPs for diagnostic use, allele-specific PCR followed by electrophoresis is usually applied [3], but simple and automated methods must be developed. SNP usually gives rise to a diallele that consists of a commonly shared sequence in a major population and a minor trait. Hybridizing a pair of single-stranded DNAs originating from both alleles yields a double-stranded DNA with a mismatched base-pair, and such DNAs are known to show different characteristics from those without a mismatch. In case a pair of bases in a double-stranded DNA cannot form hydrogen bonds between them, the thermal stability of the double strands becomes lower than that without mismatch. As a result, the double-stranded DNAs with the mismatch are dissociated at lower temperature than those without mismatch. This decrease in the dissociation temperature, i.e. the melting temperature, is usually too small to detect SNP in homogeneous liquid systems.

Affinity chromatography utilizing DNA or RNA coupled columns has already been developed for analysis and separation of DNA, RNA, nucleotide-binding proteins and other molecules [4, 5]. In affinity chromatography using DNA or RNA coupled

columns, target molecules are usually eluted by means of a continuous or stepwise change in pH or the ionic strength of the elution buffer.

However, target molecules can also be eluted by raising column temperature. By affinity chromatography using a single-stranded DNA with a complementary sequence to one of the SNP alleles, it might be possible to detect the difference in the melting temperature caused by the SNP as two separate elution peaks by temperature gradient elution. Moreover, this bioaffinity-based method has the advantage that SNPs can be detected without purification of a fragmented, and if necessary PCR-amplified, genome, and thus it may be used for automated detection of SNPs.

In this work we developed an affinity chromatographic method utilizing immobilized single-stranded DNAs and temperature gradient elution for easy and rapid SNP detection. The elution behavior of DNAs with and without SNP was experimentally and theoretically studied.

## **2. Materials and Methods**

### **2.1 Materials**

Commercially synthesized single-stranded DNAs of 25 and 50 mer were used in the present work. These DNA sequences, shown in **Table 1**, were derived from a gene, including the 248th codon, of tumor suppressor protein TP53 [1]. Five pairs of 25 mer single-strand DNAs, in which one pair is fully complementary, and four pairs had a mismatch at the 3rd, 5th, 7th or 12th position, were used to study the effect of mismatched position on the melting temperature in a homogeneous liquid system. The 5' terminus of the 50 mer DNA (50mer-c-R248R) was aminated and coupled on CNBr-activated Sepharose 4 Fast Flow (Amersham Biosciences, Uppsala, Sweden) as a single-stranded DNA ligand. A fully complementary 25 mer DNA (25mer-R248R) with the underlined portion of the 50mer-c-R248R and a single-base mutated DNA (25mer-R248W) were hybridized with the DNA ligand and dissociated by temperature gradient elution. All other chemicals used were of reagent grade.

### **2.2 Hybridization of DNA strands and measurement of melting temperature in liquid**

Double-stranded DNAs were prepared as follows. One of a pair of oligonucleotides (150 pmol) was mixed with the same amount of its complementary nucleotide in 50  $\mu$ L of NEBuffer 4 (50 mM potassium acetate, 20 mM tris-(hydroxymethyl) aminomethane, 10 mM magnesium acetate tetrahydrate and 1 mM DTT, pH 7.9). To anneal the two oligonucleotides, the mixture was incubated firstly at

94°C for 1 min, then at 55°C for 5 min and finally cooled to 4°C. After this annealing step, 50 µL of the mixture was diluted with the buffer to 250 µL (final concentration of 0.6 µM).

The melting temperature  $T_m$  of the double-stranded DNAs was determined by use of a spectrophotometer equipped with a temperature-controlled cell (S-1700, Shimadzu, Kyoto, Japan). The absorbance of DNA dissolved in the buffer was measured at 260 nm under an increasing temperature gradient (40 - 94°C, 0.5°C/min). Melting curves obtained were analyzed by the conventional two-point average method to obtain the melting temperature.

### 2.3 Measurement of elution profiles

**Figure 1** shows a schematic diagram of the experimental apparatus. The single-stranded fully complementary DNA (50 pmol) was dissolved in 100 µL of a Tris-buffer (0.5 M NaCl, 0.1 M MgCl<sub>2</sub>, 0.1 M Tris-HCl, pH 7.4) and hybridized with the ligand DNA coupled on Sepharose gel (100 µL) at room temperature for 20 min. The concentration of the DNA ligand coupled was 1.26 nmol/mL-gel. After hybridization, the gel was packed in a column (i.d. = 0.5 cm) and washed with the same buffer. The column was placed in a temperature-controlled water bath (RE307, LAUDA, Lauda-Königshofen, Germany) at 54°C and the buffer solution was supplied to the column with a micro pump (LC-10ADvpµ, Shimadzu, Kyoto, Japan) for equilibration. A part of the PETF tube (about 50 cm, i.d. = 0.25 mm, o.d. = 1.6 mm) connecting between the pump and the inlet of the column was immersed in the water bath to raise

the temperature of the solution supplied to the column. The double-stranded DNA was then dissociated by raising column temperature in the water bath. The absorbance of the effluent solution from the column was continuously measured at 260 nm with a UV detector (SPD-10Avp, Shimadzu).

The effects of the packed gel volume, flow rate of the eluent and heating rate of the column on elution profiles were studied under the following conditions:

- (a) Packed volume: 100  $\mu\text{L}$ , 200  $\mu\text{L}$ , 300  $\mu\text{L}$ , at constant flow rate of 50  $\mu\text{L}/\text{min}$  and heating rate of 0.5°C/min.
- (b) Flow rate: 30  $\mu\text{L}/\text{min}$ , 50  $\mu\text{L}/\text{min}$ , 100  $\mu\text{L}/\text{min}$ , at constant packed volume of 100  $\mu\text{L}$  and heating rate of 0.5°C/min.
- (c) Heating rate: 0.5°C/min, 1.0°C/min, 2.0°C/min, at constant packed volume of 100  $\mu\text{L}$  and flow rate of 50  $\mu\text{L}/\text{min}$ .

To study the effects of the ratio of the single-base mismatched DNA (25mer-R248W) to the fully complementary DNA (25mer-R248R) on the elution profiles, a mixture of these DNAs was dissolved in 100  $\mu\text{L}$  of the buffer solution at a ratio of 1:1, 1:9 or 9:1 (50 pmol as a total) and hybridized with 100  $\mu\text{L}$  of gel by the procedures stated above. In these experiments, elution profiles were obtained by use of 100  $\mu\text{L}$  of gel at a flow rate of 50  $\mu\text{L}/\text{min}$  and a heating rate of 0.5°C/min.

## **2.4 Prediction of elution profiles**

A basic material balance equation for the fully complementary DNA (25mer-R248R) on a volume element of differential height in a packed column is given

with the assumptions of a uniform velocity distribution over the cross section of the column as follows:

$$\frac{\partial C}{\partial t} = -u \frac{\partial C}{\partial z} - \frac{1-\varepsilon}{\varepsilon} \frac{\partial \overline{C}_s}{\partial t} \quad (1)$$

where  $C$  (mol/mL-mobile phase) is the concentration of dissociated 25mer-R248R DNA in the mobile phase,  $t$  (s) time,  $u$  (cm/s) the linear velocity of the eluent through the void of the packed column,  $z$  (cm) the distance from the top of the packed bed,  $\varepsilon$  (-) the void fraction of the packed bed, and  $\overline{C}_s$  (mol/mL-stationary phase) the total concentration of 25mer-R248R DNA in the stationary phase. The effects of the axial eddy and molecular diffusion on elution profiles can be neglected in the affinity chromatography under the present conditions.

The rate of DNA transfer from the stationary phase to the mobile phase can be expressed in terms of the averaged overall volumetric coefficient of mass transfer,

$$\overline{K_{of} a_p} : \quad \frac{\partial \overline{C}_s}{\partial t} = \overline{K_{of} a_p} (\overline{C}_p - C) \quad (2)$$

where  $\overline{C}_p$  (mol/mL-stationary phase) is the concentration of dissociated 25mer-R248R DNA remaining in the stationary phase, which was calculated from the degree of DNA dissociation  $\theta_d$  and the material balance for dissociated DNA between stationary and mobile phases.

The proportion of DNA dissociated from the DNA ligand in the stationary phase at a specific temperature was estimated by use of thermodynamic parameters determined

from the melting curve of hybridized DNA dissolved in the Tris-buffer (pH 7.4). The degree of DNA dissociation  $\theta_d$  was calculated using the following equation, as shown in

**Fig. 2.**

$$\theta_d(T) = \frac{A(T) - A_{pre}(T)}{A_{post}(T) - A_{pre}(T)} \quad (3)$$

where  $A(T)$  is the absorbance of the sample at temperature  $T$ , and  $A_{pre}(T)$  and  $A_{post}(T)$  are the absorbances at temperature  $T$  on the pretransition and posttransition linear baselines of the melting curve, respectively. Since the amount of the DNA ligand in the stationary phase was much higher than that of the hybridized DNA strand, the equilibrium constant for dissociation of the hybridized DNA from the ligand  $K_{eq}$  is given based on the Van 't Hoff equation,

$$\ln K_{eq}(T) = -\frac{\Delta H^0}{R} \cdot \frac{1}{T} + \text{const.} = \ln \frac{\theta_d(T)}{1 - \theta_d(T)} \quad (4)$$

where  $\Delta H^0$  is standard enthalpy change and  $R$  the gas constant. When  $\Delta H^0$  is independent of temperature, a plot of  $\ln\{\theta_d(T)/(1-\theta_d(T))\}$  against  $1/T$  gives a straight line, and the value of  $\Delta H^0$  is determined from the slope. Equation (4) gives the temperature dependence of the equilibrium constant, and can be used for calculation of the degree of DNA dissociation at a specific temperature.

Elution profiles shown in latter sections were calculated numerically by the finite difference method using Eqs. (1) – (4). The averaged overall volumetric coefficient

$\overline{K_{of} a_p}$  was determined by fitting a calculated curve to an experimental elution curve of the 25 mer-R248R DNA (solid curve in Fig. 5) as 0.036 1/s at 80°C, and the void fraction of 0.3 was used for the numerical calculation of elution profiles. This value of

the volumetric coefficient was almost the same as the reported value (0.01 1/s) after correction for temperature and viscosity [6].

### 3. Results and Discussion

#### 3.1 Effect of mismatch position on the melting temperature

We firstly examined the effects of mismatched position on the melting temperature of the double-stranded DNAs with a mismatched base-pair. **Figure 3** shows the difference of the melting temperature between fully complementary and single mismatched double-stranded DNAs. The temperature difference  $\Delta T_m$  increased when the mismatched pair was close to the center of the DNA. In this case, the longer completely matched portion of the pair of DNA strands was shorter than when the mismatch was close to either end. These results show that the  $\Delta T_m$  can be controlled by the position of a mismatched pair, as well as the length of DNA strands and the GC content [7]. In practical case for SNP detection, a single-stranded DNA ligand with a suitable length can be designed against a specific portion of a target DNA, which may be longer than the ligand but interacts with the ligand at the specific portion.

#### 3.2 Determination of thermodynamic parameter from melting curve

From the measured value of DNA dissociation between the 50 mer and the fully complementary 25 mer in the Tris-buffer, the equilibrium constants were calculated at different temperatures and plotted against the inverse of absolute temperature, as shown in **Fig. 4**. According to Eq. (4), this line gave the temperature dependence of the equilibrium constant of the DNA dissociation, and a  $\Delta H^0$  value of 8470 (J/mol) was obtained. Because of the differences in the degree of freedom and the density between DNA strands in homogeneous solution and those coupled with ligands on the gel, the

melting temperature of the double-stranded DNA formed on the gel was slightly higher. Therefore, to fit the peak tops of dissociation profiles from the DNA coupled with ligands on the gel, we shifted the obtained straight line parallel to the x-axis and used it for estimation of elution profiles.

### **3.3 Elution behavior of single-stranded DNA from ligand DNA**

#### **(a) Effect of packed volume on elution behavior**

**Figure 5** shows a typical elution profile of the fully complementary DNA from the ligand DNA immobilized on Sepharose 4 Fast Flow (solid curve) and also the effect of the packed gel volume on elution profiles. The temperature range in which the DNA dissociated from the DNA ligand was slightly higher than that in the homogeneous solution. The profiles of the eluted DNA were not symmetrical, that is, the elution profiles ascended gradually and descended rapidly, because the dissociation of DNA was accelerated at higher temperature, as shown in Fig. 2.

The driving force for mass transfer of dissociated DNA from the stationary (gel) phase to the mobile phase was the concentration difference between these two phases. As the gel volume increased, the concentration of dissociated DNA in the mobile phase increased along the axis of the column. Therefore, the driving force for mass transfer decreased with increase in the bed height, and as a consequence the peak tops of the elution profiles were retarded to the higher temperature.

#### **(b) Effect of flow rate on elution behavior**

**Figure 6** shows the effect of the flow rate on elution profiles. With increase in the

flow rate, the DNA concentration in the effluent solution decreased. On the other hand, the temperature of the peak tops became lower with increase in the flow rate, since the driving force for mass transfer between the mobile phase and the gel phase increased, and the mass transfer coefficient also increased with the flow rate. These factors accelerated transport of dissociated DNA from the gel phase.

### **(c) Effect of heating rate on elution behavior**

The effect of the heating rate in the temperature-controlled water bath on elution profiles is shown in **Fig. 7**. With increase in the heating rate, the elution profiles were retarded. Because of the resistance for heat transfer in the column, the lag in the temperature rise of the packed beads might retard dissociation of the DNA strands from the ligand DNA.

## **3.4 Comparison of elution behaviors of fully complementary and single-base mismatched DNAs**

**Figure 8** shows the elution profiles from the affinity column of complementary and single-base mismatched DNAs mixed at different ratios. The difference in thermal stability between the DNA strands with or without the mismatch resulted in elution profiles having two peaks. The first peak originated from the single-base mismatched strand, which was less thermostable and dissociated from the ligand DNA at lower temperature. With increase in the proportion of the complementary DNA, the temperature difference between two tops of the elution profiles increased, which demonstrated these two strands were interacting with the ligand in the process of

dissociation.

The fully complementary DNA or the single-base mismatched DNA contained at 10% of the total DNAs was detected as a shoulder-like peak, as shown in Fig. 8, at the later part or earlier part of the elution profile. Thus, the single-base mismatched DNA can be distinguished from the fully complementary DNA used as a control, and use of a small amount of the mismatched DNA will be suitable for practical SNP detection. As shown in 3.3, decreasing the flow rate and/or increasing the heating rate increased the peak height, and thus showed high sensitivity. However, they broadened the peak width and affected the resolution. Therefore, to decrease the required amount of the mismatched DNA, detection conditions, such as the mixing ratio, the liquid flow rate and the temperature gradient, should be optimized.

### 3.5 Comparisons between experimental and calculated elution profiles

In Figs. 5, 6 and 7, experimentally obtained elution profiles (lines) are compared with calculated elution profiles, shown by symbols. In the calculation of the elution profiles at flow rates different from 50  $\mu\text{L}/\text{min}$ , the volumetric mass transfer coefficient was assumed to vary in proportion to the 1/2-power of the flow rate. To compensate for the delay in the temperature rise caused by the resistance for heat transfer in the column, a first-order lag element was introduced to calculate the elution profile for heating rates of 1.0 and 2.0  $^{\circ}\text{C}/\text{min}$ . The calculated time  $t_{cal}$  was converted to the compensated time  $t_{com}$  by the following equation:

$$t_{com} = K \left\{ t_{cal} - \tau \left( 1 - e^{-t_{cal}/\tau} \right) \right\} \quad (5)$$

where  $K$  is the steady-state gain and  $\tau$  the time constant. The values of 1.08 and 0.18 were used for  $K$  (-) and  $\tau$  (min), respectively.

The good agreement found between experimental and calculated elution profiles showed that the present model based on the mass and heat transfer rates could be used to estimate the elution profiles of the single-stranded DNAs dissociated from the DNA ligand in the temperature gradient affinity chromatography. This calculation method is very useful to optimize the detection conditions, and thus to improve the sensitivity of SNP detection by this affinity-based method. At present, it is possible to detect SNPs in DNA samples of 1 pmol under optimized conditions (data will be presented in a later paper), but further improvement of the sensitivity will be necessary to detect SNPs without PCR amplification.

## Nomenclature

|                         |  |
|-------------------------|--|
| $A(T)$                  | absorbance of DNA solution at temperature $T$ (-)  |
| $A_{pre}(T)$            | absorbance at temperature $T$ on the pretransition linear baseline of the melting curve (-)  |
| $A_{post}(T)$           | absorbance at temperature $T$ on the posttransition linear baseline of the melting curve (-) |
| $C$                     | concentration of dissociated 25mer-R248R DNA in mobile phase (mol/mL)                        |
| $\overline{C}_s$        | total concentration of 25mer-R248R DNA in stationary phase (mol/mL)                          |
| $\overline{C}_p$        | concentration of dissociated 25mer-R248R DNA remaining in stationary phase (mol/mL)          |
| $\Delta H^0$            | standard enthalpy change (J/mol)   |
| $K$                     | steady-state gain (-)  |
| $K_{eq}$                | equilibrium constant for dissociation of the hybridized DNA from the ligand (-)              |
| $\overline{K_{of} a_p}$ | averaged overall volumetric coefficient of mass transfer (/s)                                |
| $R$                     | gas constant = 8.3144 (J/(mol·K))  |
| $t$                     | time (s)   |
| $T$                     | temperature (°C)   |
| $t_{cal}$               | calculated time (min)  |
| $t_{com}$               | compensated time (min)   |
| $T_m$                   | melting temperature (°C)   |

|               |   |
|---------------|---|
| $\Delta T_m$  | difference in melting temperature between fully complementary and single mismatched double-stranded DNAs (°C) |
| $u$           | linear velocity of a mobile phase through the void of the column (cm/s)                                       |
| $z$           | distance from the top of the packed bed (cm)  |
| $\varepsilon$ | void fraction of packed bed (-)   |
| $\theta_d$    | proportion of DNAs dissociated from the DNA ligand in the stationary phase (-)                                |
| $\tau$        | time constant (min)   |

## References

- [1] S.M. Morris, *Mutat. Res.* 511 (2002) 45.
- [2] M. Pirmohamed, B.K. Park, *Trends Pharmacol. Sci.* 22 (2001) 298.
- [3] D.Y. Wu, L. Ugozzoli, B.K. Pal, R.B. Wallace, *Proc. Natl. Acad. Sci. USA* 86 (1989) 2757.
- [4] T.S. Roming, C. Bell, D.W. Drolet, *J. Chromatogr. B* 731 (1999) 275.
- [5] Q. Deng, I. German, D. Buchanan, R.T. Kennedy, *Anal. Chem.* 73 (2001) 5415.
- [6] S. Katoh, E. Sada, *J Chem. Eng. Japan* 13 (1980) 151.
- [7] T. Katsuda, K. Nishijima, M. Kamura, Z.S.M. Hossain, S. Katoh, in *Conference Proceedings 10th the Asian Pacific Confederation of Chemical Engineering Congress*. The Society of Chemical Engineers, Japan, 2004, 1P-01-009.

## Figure captions

Fig. 1. A schematic diagram of the experimental apparatus.

Fig. 2. Determination of the proportion of DNAs dissociated from the ligand DNAs.

The solid line is the melting curve of the hybridized double-stranded DNA consisting of 50mer-c-R248R and 25mer-R248R single-stranded DNAs. The dashed line shows the proportion of dissociated DNA calculated by Eq. (3).

Fig. 3. Effects of mismatched position in a double-stranded DNA on the melting temperature difference.

Fig. 4. Plot of  $\ln K_{eq}$  against  $1/T$ . The equilibrium constant at each temperature was calculated from  $\theta_d(T)$  by Eq. (4). The straight line was obtained by linear regression.

Fig. 5. Elution profiles obtained with different column volumes. Lines, elution profiles obtained experimentally; symbols, calculated values.

Bed volume: closed diamond, 100  $\mu\text{L}$ ; open square, 200  $\mu\text{L}$ ; open circle, 300  $\mu\text{L}$ . The flow and heating rates were 50  $\mu\text{L}/\text{min}$  and 0.5°C/min, respectively (Condition (a) in Materials and Methods).

Fig. 6. Elution profiles under different flow rates. Lines, elution profiles obtained experimentally; symbols, calculated values.

Flow rate: closed diamond, 50  $\mu\text{L}/\text{min}$ ; open square, 100  $\mu\text{L}/\text{min}$ ; open circle, 30  $\mu\text{L}/\text{min}$ .

The column volume and heating rate were 100  $\mu\text{L}$  and  $0.5^\circ\text{C}/\text{min}$ , respectively

(Condition (b) in Materials and Methods).

Fig. 7. Elution profiles at different heating rates. Lines, elution profiles obtained experimentally; symbols, calculated values. Heating rate: closed diamond,  $0.5^\circ\text{C}/\text{min}$ ; open square,  $1.0^\circ\text{C}/\text{min}$ ; open circle,  $2.0^\circ\text{C}/\text{min}$ .

The column volume and flow rate were 100  $\mu\text{L}$  and 50  $\mu\text{L}/\text{min}$ , respectively (Condition (c) in Materials and Methods).

Fig. 8. Elution profiles of complementary and single-base mismatched DNAs mixed at different ratios.

Proportion of fully complementary DNA: chain line, 10%; solid line, 50%; dotted line, 90%. The column volume, flow rate and heating rate were 100  $\mu\text{L}$ , 50  $\mu\text{L}/\text{min}$  and  $0.5^\circ\text{C}/\text{min}$ , respectively.

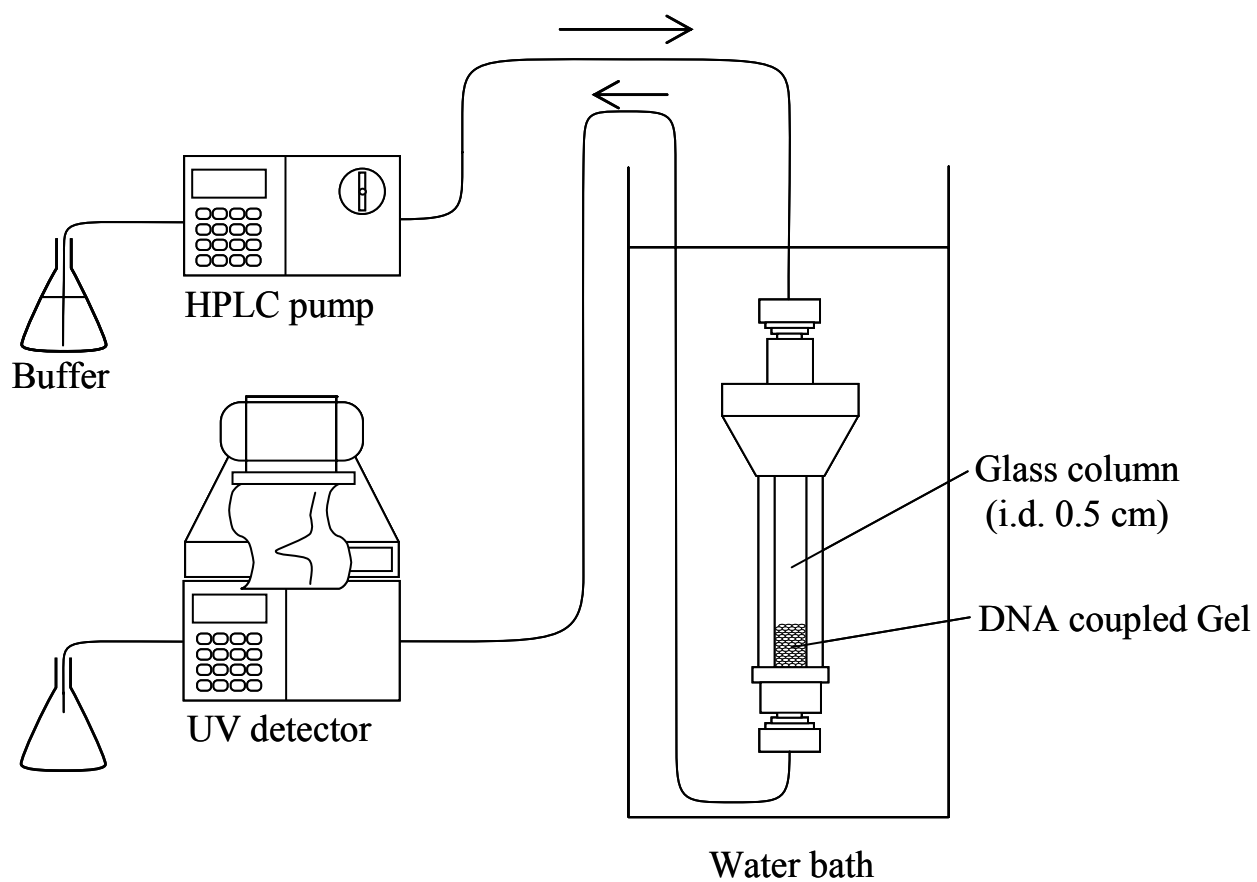


Fig. 1. A schematic diagram of the experimental apparatus.

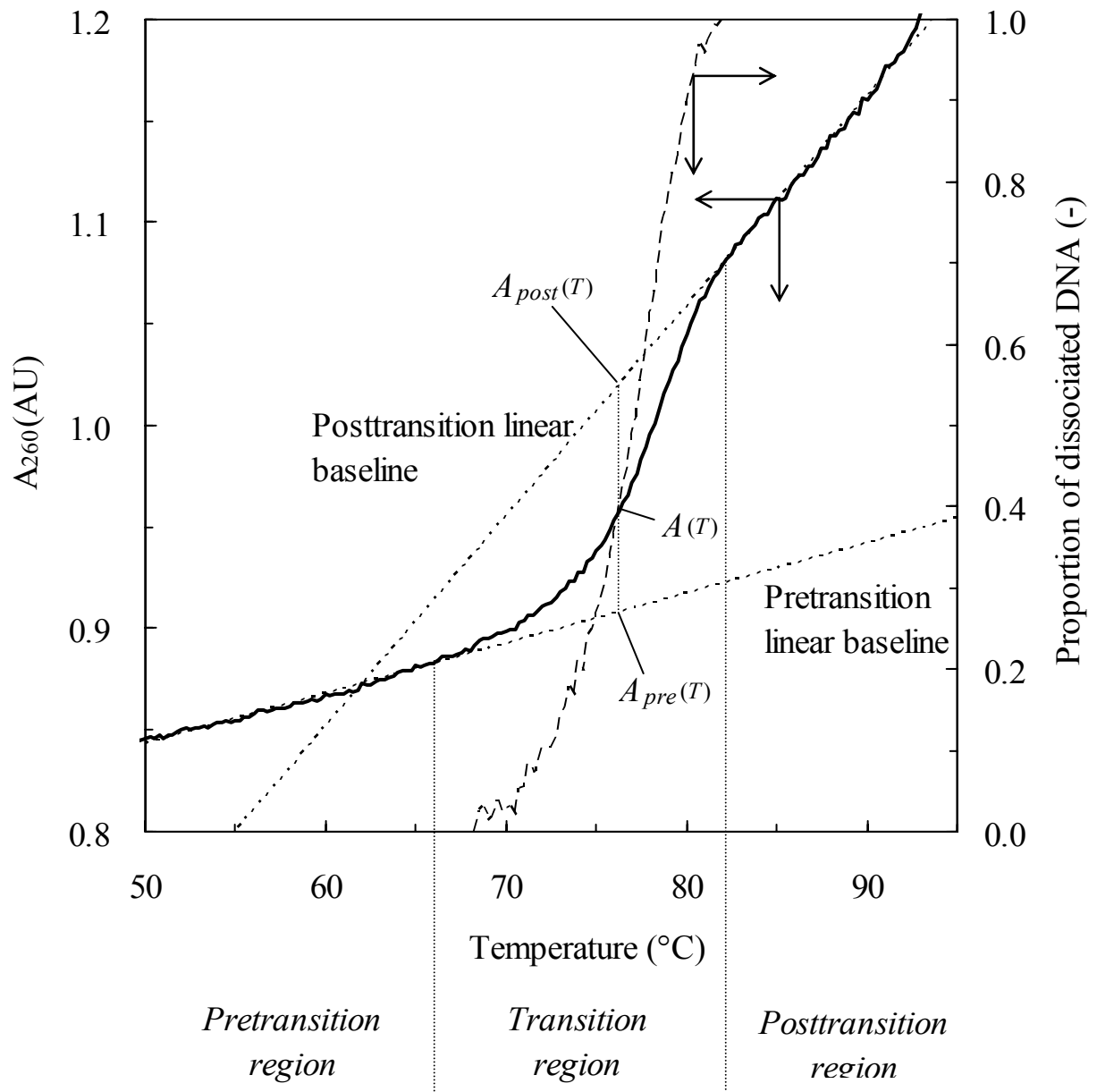


Fig. 2. Determination of the proportion of DNAs dissociated from the ligand DNAs. The solid line is the melting curve of the hybridized double-stranded DNA consisting of 50mer-c-R248R and 25mer-R248R single-stranded DNAs. The dashed line shows the proportion of dissociated DNA calculated by Eq. (3).

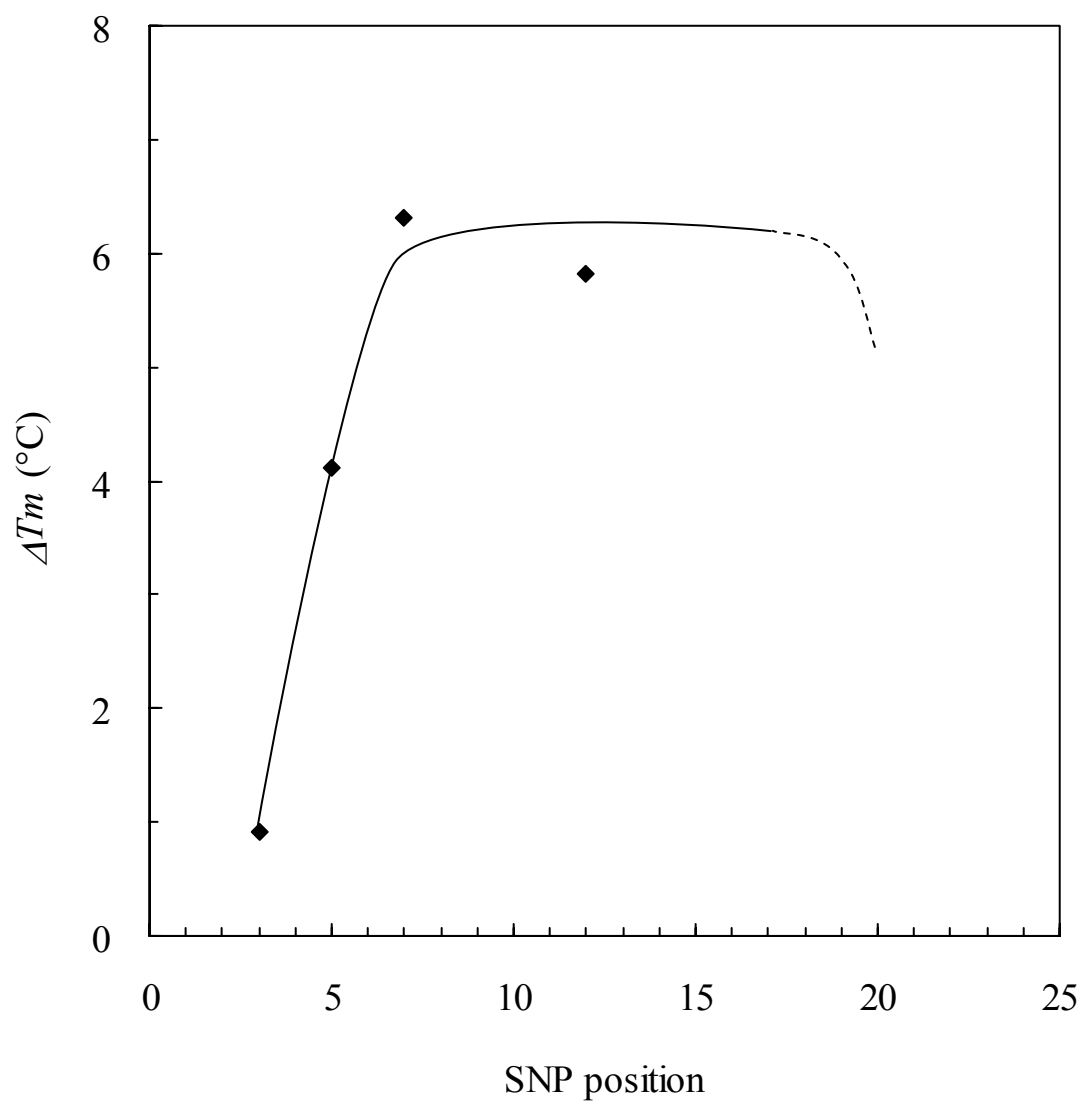


Fig. 3. Effects of mismatched position in a double-stranded DNA on the melting temperature difference.

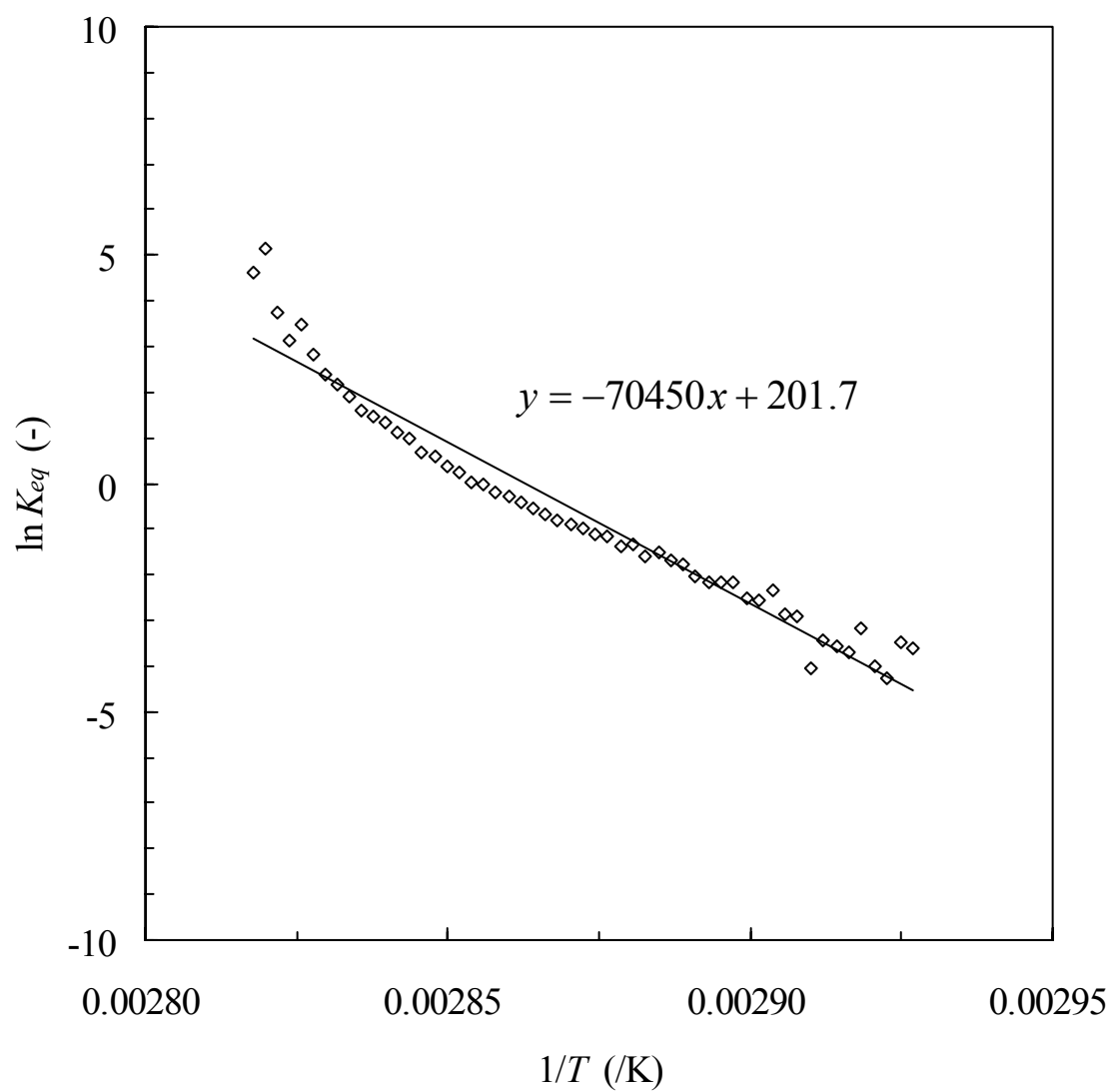


Fig. 4. Plot of  $\ln K_{eq}$  against  $1/T$ . The equilibrium constant at each temperature was calculated from  $\theta_d(T)$  by Eq. (4). The straight line was obtained by linear regression.

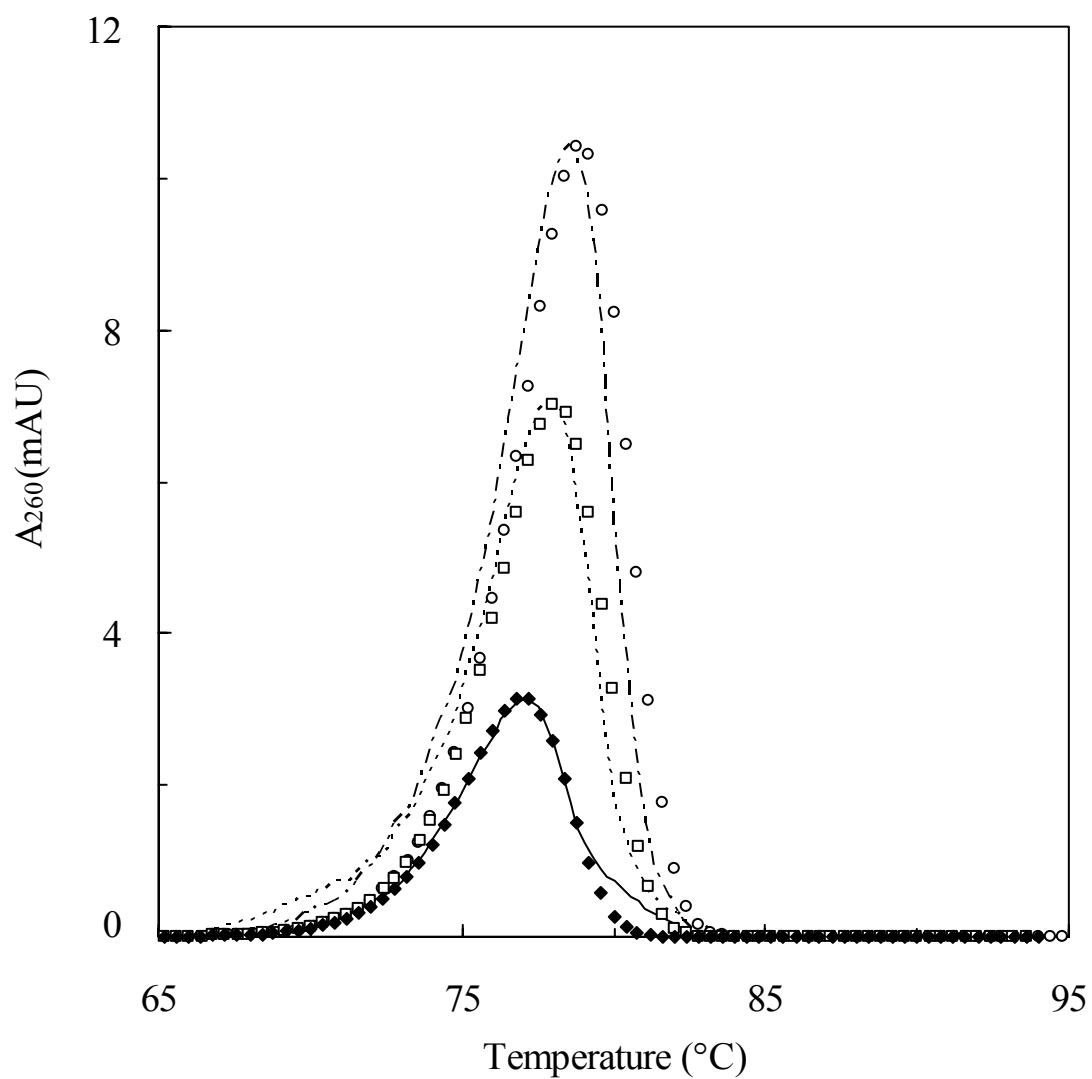


Fig. 5. Elution profiles obtained with different column volumes. Lines, elution profiles obtained experimentally; symbols, calculated values. Bed volume: closed diamond, 100  $\mu\text{L}$ ; open square, 200  $\mu\text{L}$ ; open circle, 300  $\mu\text{L}$ . The flow and heating rates were 50  $\mu\text{L}/\text{min}$  and  $0.5^\circ\text{C}/\text{min}$ , respectively (Condition (a) in Materials and Methods).

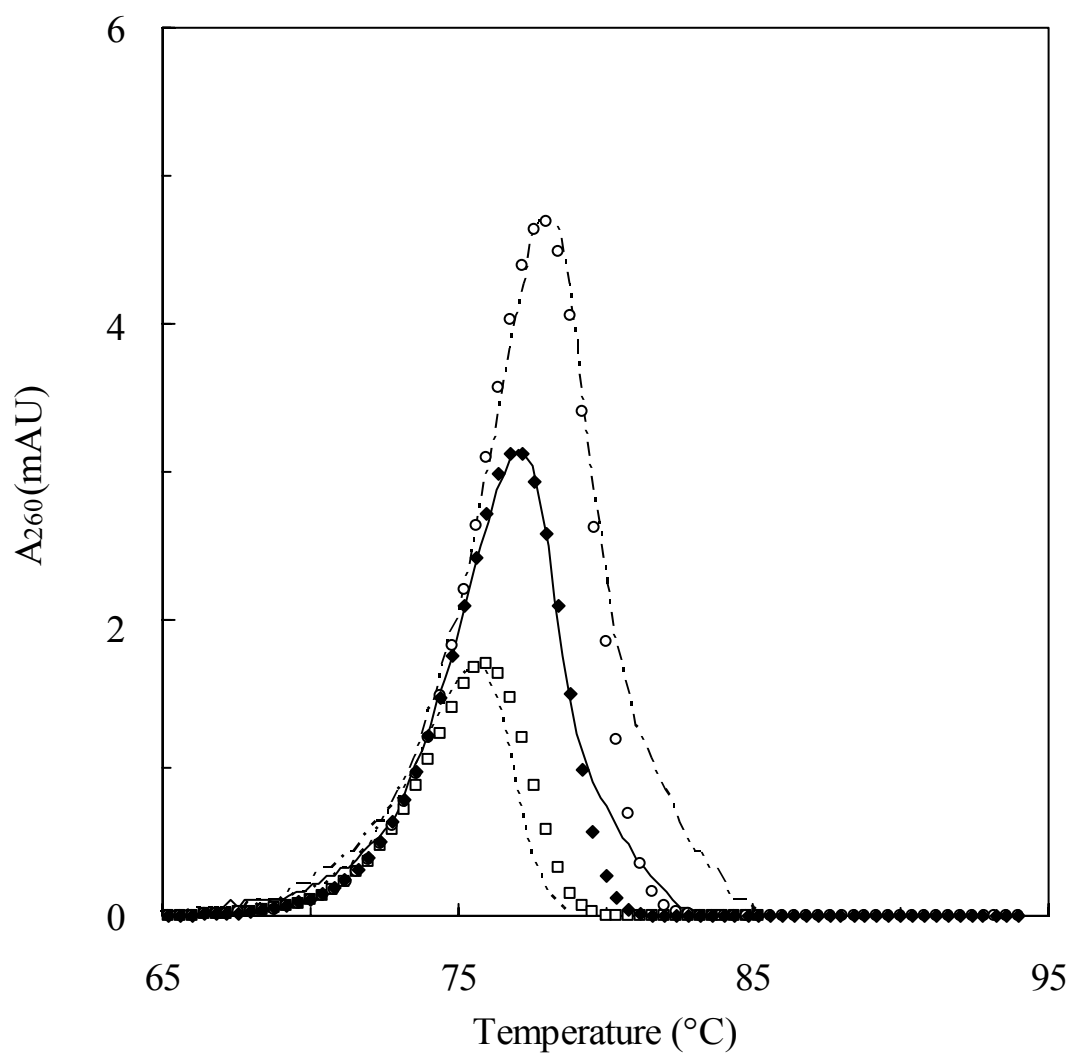


Fig. 6. Elution profiles under different flow rates. Lines, elution profiles obtained experimentally; symbols, calculated values. Flow rate: closed diamond, 50  $\mu\text{L}/\text{min}$ ; open square, 100  $\mu\text{L}/\text{min}$ ; open circle, 30  $\mu\text{L}/\text{min}$ . The column volume and heating rate were 100  $\mu\text{L}$  and 0.5 $^{\circ}\text{C}/\text{min}$ , respectively (Condition (b) in Materials and Methods).

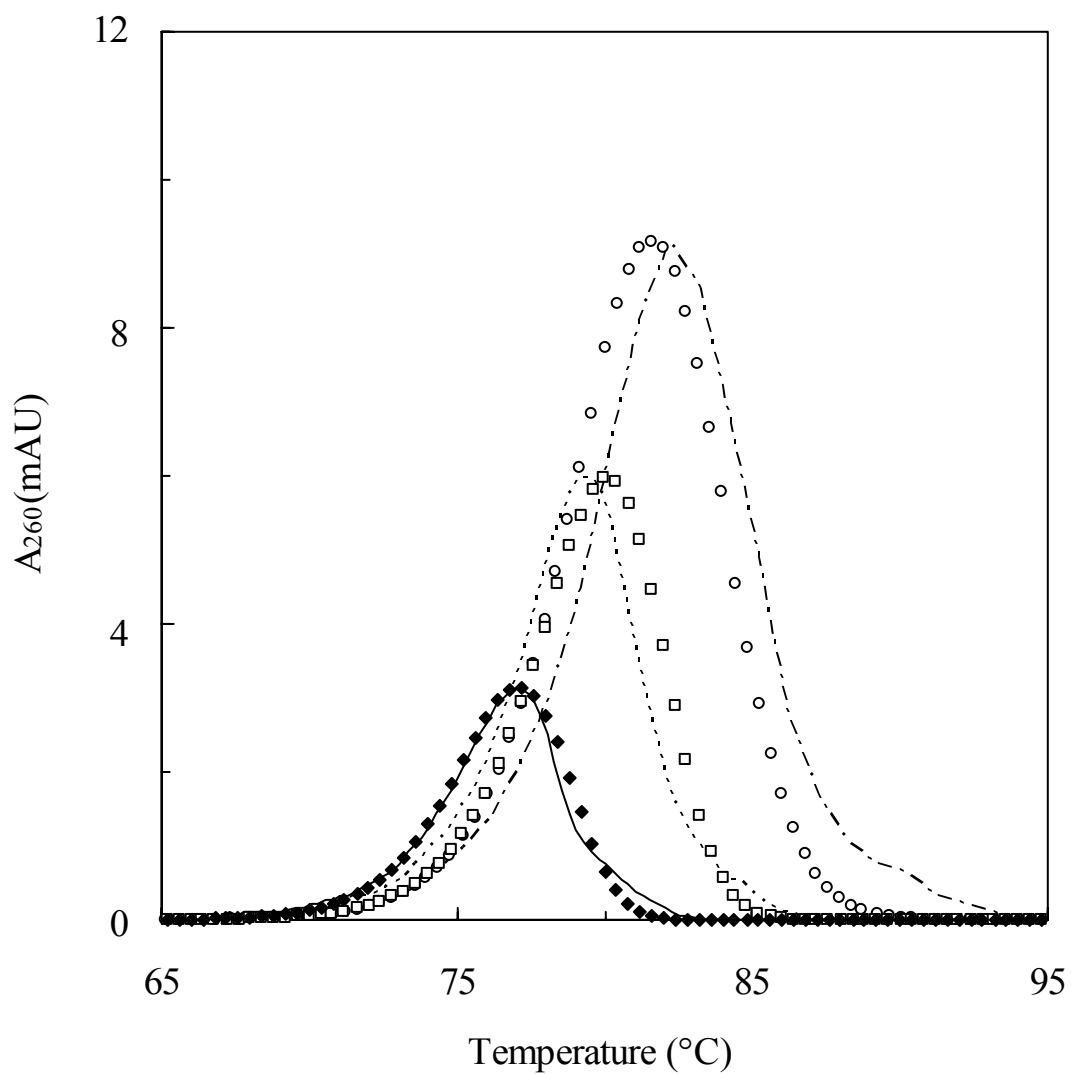


Fig. 7. Elution profiles at different heating rates. Lines, elution profiles obtained experimentally; symbols, calculated values. Heating rate: closed diamond, 0.5°C/min; open square, 1.0°C/min; open circle, 2.0°C/min. The column volume and flow rate were 100  $\mu$ L and 50  $\mu$ L/min, respectively (Condition (c) in Materials and Methods).

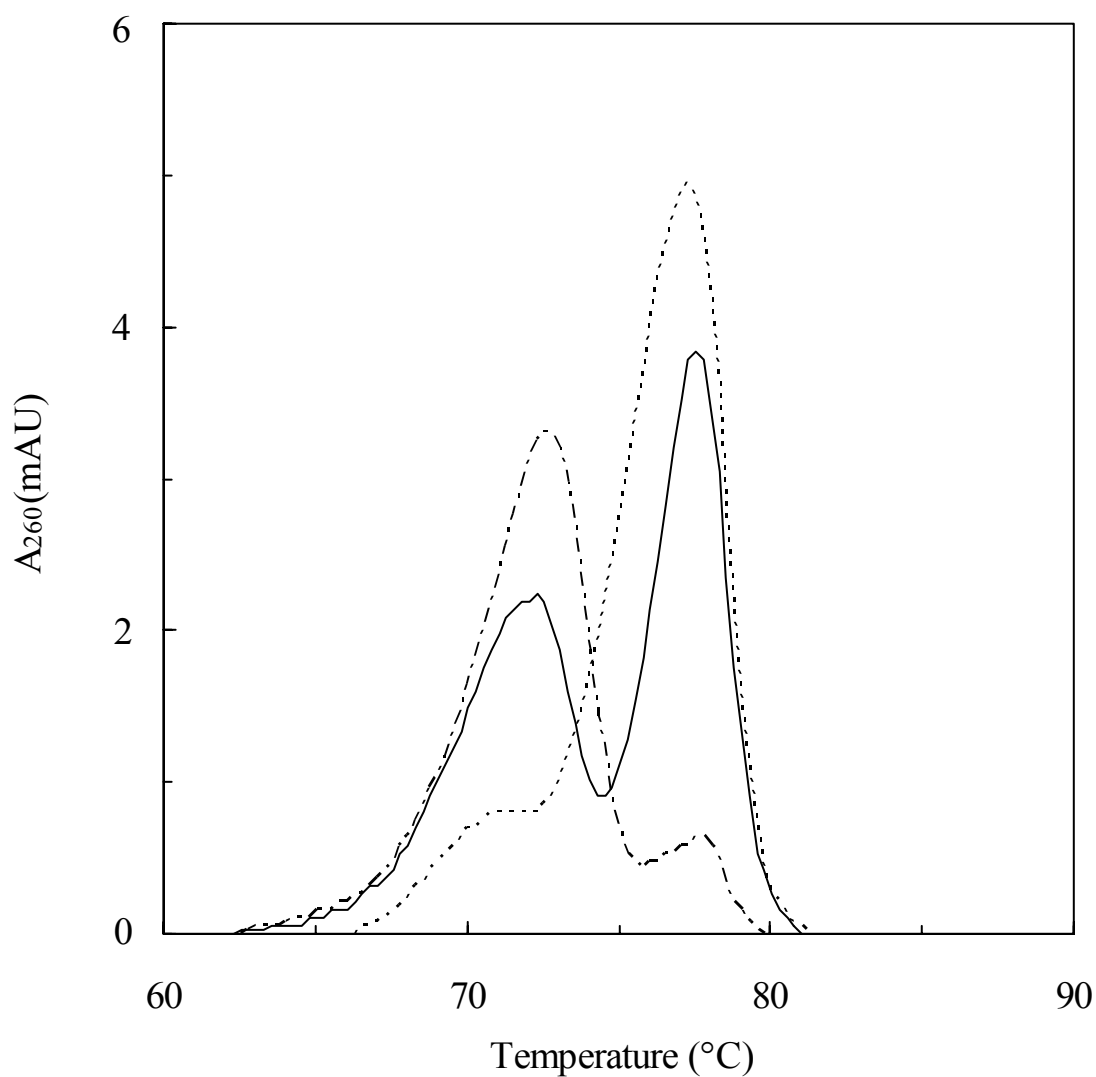


Fig. 8. Elution profiles of complementary and single-base mismatched DNAs mixed at different ratios. Proportion of fully complementary DNA: chain line, 10%; solid line, 50%; dotted line, 90%. The column volume, flow rate and heating rate were 100  $\mu$ L, 50  $\mu$ L/min and 0.5°C/min, respectively.